Experimental Thermal and Fluid Science 46 (2013) 139–150

Contents lists available at SciVerse ScienceDirect

Experimental Thermal and Fluid Science

journal homepage: www.elsevier.com/locate/etfs

Experimental and numerical investigation of unsteady behaviour in the near-field of pure thermal planar plumes

T. Hattori [a,*], N. Bartos [a], S.E. Norris [b], M.P. Kirkpatrick [a], S.W. Armfield [a]

[a] School of Aerospace, Mechanical and Mechatronic Engineering, The University of Sydney, Sydney, NSW 2006, Australia
[b] Department of Mechanical Engineering, The University of Auckland, Auckland, New Zealand

ARTICLE INFO

Article history:
Received 15 August 2012
Received in revised form 8 December 2012
Accepted 13 December 2012
Available online 21 December 2012

Keywords:
Natural convection
Direct numerical simulation
Shadowgraph
Particle image velocimetry
Rayleigh–Taylor instability

ABSTRACT

A near-field, unsteady buoyant plume exhibits puffing behaviour, characterised by the periodic formation of large-scale vortical structures (puffs). It has been observed in numerical simulations of pure thermal plumes with a finite area source that the periodic formation of puffs is associated with an instability of the lapping flow that develops over the heated region away from the plume centreline, producing bulge-like structures. Experiments using a shadowgraph technique and two-dimensional, two-component particle image velocimetry are conducted to validate our numerical results for the near-field, unsteady behaviours of a pure thermal planar plume, with water as the working fluid. The formations of bulges in the lapping flow and associated puffs are also observed in transient flow fields obtained in the experiments. Further, quantitative comparison of mean velocity field and oscillation frequencies obtained in the experiments and numerical simulation shows reasonable agreement. This experimental study confirms the important effect of the lapping flow instability on the near-field unsteady behaviour, which has been highlighted in numerical simulations.

1. Introduction

The near-field, transitional behaviour of a buoyant plume is characterised by the periodic formation of large-scale vortical structures (puffs). While most related studies considered forced plume configurations [1–7], in this investigation we consider pure thermal plumes, which have received relatively little attention [8].

In the near-field of a finite area source of buoyancy, it is known that a horizontal inward moving boundary layer flow, the lapping flow, as shown in Fig. 1, forms away from the plume centreline, which turns upward in the central region and feeds the buoyant fluid into the vertical ascending column [9]. Plourde et al. [8], reporting on the numerical study of a pure thermal axisymmetric plume with air as the working fluid, observed a periodic puffing that is associated with an instability of the lapping flow, forming a thermal plumelet (bulge), which eventually merges with and surrounds the central ascending column. In our recent study [10], this near-field behaviour was numerically studied for a pure thermal planar plume with a Prandtl number, Pr, of 7.0. To investigate the lapping flow instability, we modelled the lapping flow adjacent to the plume source by a channel flow with a heated floor section, providing an additional control parameter, the channel inlet velocity, that varies the lapping flow velocity. A Froude number, Fr, was defined as a measure of the lapping flow velocity. Bulge structures were also observed to form in this flow above a critical Reynolds number, Re, and below a critical Fr. With increasing Fr, the bulge was found to form further downstream, hence it was assumed that an increase in Fr reduces the spatial growth rate of the Rayleigh–Taylor instability. Further, the oscillation frequencies in the plume stem were found to be closely correlated to those in the lapping flow, which suggests the existence of a convective-type instability of the near-field flow. A similar bulge forming instability over the heated region of the floor, with associated puffing, was also observed in a study of the transitional ventilated filling box flow reported in [11].

All of the results discussed above were obtained by numerical simulation only. The aim of this study is to provide the validation for the puffing behaviour associated with the bulge formation in the lapping flow by experiment using a shadowgraph technique and two-dimensional, two-component particle image velocimetry (2D2C-PIV). In Section 2, the numerical method is discussed. In Section 3, the experimental methods used for both shadowgraphy and 2D2C-PIV are discussed. The numerical and experimental results are presented and compared in Section 4, followed by conclusions in Section 5.

* Corresponding author. Tel.: +61 2 9351 7142; fax: +61 2 9351 7060.
E-mail addresses: tae.hattori@sydney.edu.au (T. Hattori), nicholas.bartos@sydney.edu.au (N. Bartos), s.norris@auckland.ac.nz (S.E. Norris), michael.kirkpatrick@sydney.edu.au (M.P. Kirkpatrick), steven.armfield@sydney.edu.au (S.W. Armfield).

0894-1777/$ - see front matter © 2012 Elsevier Inc. All rights reserved.
http://dx.doi.org/10.1016/j.expthermflusci.2012.12.005

Nomenclature

g^*	Gravitational acceleration (m/s^2)
Pr	Prandtl number (non-dimensional, $\mathrm{Pr} = \nu^*/\kappa^*$)
Re	Reynolds number (non-dimensional, $\mathrm{Re} = U^*L^*/\nu^*$)
St	frequency (non-dimensional, $\mathrm{St} = f^*L^*/U^*$)
f^*	frequency (Hz)
u_i	velocity (non-dimensional, $u_i = u_i^*/U^*$)
t	time (non-dimensional, $t = t^*U^*/L^*$)
x_i	coordinates (non-dimensional, $x_i = x_i^*/L^*$)
p	pressure perturbation (non-dimensional, $p = p^*/\rho^*U^{*2}$)
T	temperature perturbation (non-dimensional, $T = (T^* - T_\infty^*)/(T_s^* - T_\infty^*)$)
T^*	local temperature (K)
T_∞^*	ambient temperature (K)
T_s^*	source temperature (K)
U^*	characteristic velocity scale (m/s, $U^* = \sqrt{g^*\beta^*(T_s^* - T_\infty^*)L^*}$)
L^*	characteristic length scale (m)
Δt	time step (non-dimensional)
Δt_l^*	time difference between laser pulses (s)
Δx_i	grid spacing in the x_i direction (non-dimensional)
N_{x_i}	number of grids in the x_i direction
ΔI^*	change in light intensity due to refractive index change
I^*	light intensity
n	refractive index
l^*	distance from a plane in the test section to the screen (m)
u_∞^*	settling velocity (m/s)
d_p^*	particle diameter (m)
c_I	the number of pixels over one side of the interrogation window
d_r^*	the size of one pixel (m)
M	magnification
U_{max}^*	the maximum flow velocity (m/s)
δ_{ij}	Kronecker delta
κ^*	thermal diffusivity (m^2/s)
ν^*	kinematic viscosity (m^2/s)
β^*	thermal expansion coefficient (1/K)
ρ_p^*	particle density (kg/m^3)
ρ_f^*	fluid density (kg/m^3)
μ_f^*	fluid dynamic viscosity (kg/ms)
*	dimensional quantity
i, j	indices for tensor notation
$\langle\rangle$	time averaging operator

2. Numerical method

The computational domain is shown in Fig. 1. The governing equations are the non-dimensional, incompressible Navier–Stokes equations with the Boussinesq approximation for buoyancy:

$$\frac{\partial u_i}{\partial t} + \frac{\partial (u_j u_i)}{\partial x_j} = -\frac{dp}{dx_i} + \frac{\partial}{\partial x_j}\left(\frac{1}{\mathrm{Re}}\frac{\partial u_i}{\partial x_j}\right) + T\delta_{i2}, \tag{1}$$

$$\frac{\partial T}{\partial t} + \frac{\partial (u_i T)}{\partial x_i} = \frac{\partial}{\partial x_i}\left(\frac{1}{\mathrm{RePr}}\frac{\partial T}{\partial x_i}\right), \tag{2}$$

$$\frac{\partial u_i}{\partial x_i} = 0, \tag{3}$$

where $i = 1,\ 2,\ 3$ and $j = 1,\ 2,\ 3$. $x_1 = x,\ x_2 = y$ and $x_3 = z$ are the coordinates as shown in Fig. 1, and t is time. $u_1 = u,\ u_2 = v$ and $u_3 = w$ are the velocity components in the $x,\ y$ and z directions, respectively. p is the pressure perturbation and T the temperature perturbation given as $T = (T^* - T_\infty^*)/(T_s^* - T_\infty^*)$, where T^* is the dimensional local temperature, T_∞^* the dimensional ambient temperature and T_s^* the dimensional source temperature. The superscript, *, is used for dimensional quantities.

Control parameters are the Reynolds and Prandtl numbers. The Reynolds number is defined as $\mathrm{Re} = U^*L^*/\nu^*$, where $U^* = \sqrt{g^*\beta^*(T_s^* - T_\infty^*)L^*}$, with L^* the plume source width, ν^* the kinematic viscosity, g^* the gravitational acceleration, and β^* is the thermal expansion coefficient. The Prandtl number is $\mathrm{Pr} = \nu^*/\kappa^*$, with κ^* the thermal diffusivity.

For the study, a non-staggered, Cartesian mesh, finite volume code was used [12]. The code is based on a fractional step method [13], with the Adams–Bashforth and Crank–Nicolson time discretisation schemes being used for the advection and diffusion terms, respectively. The spatial discretisations for the diffusion terms in Eqs. (1) and (2) and the advection terms in Eq. (1) used second-order central differencing, while for the advection terms in Eq. (2) fourth-order central differencing with the ULTRA (Universal Limiter for Tight Resolution and Accuracy) flux limiter [14] was used. The Strongly Implicit Procedure (SIP) [15] was used for Eqs. (1) and (2), and the Bi-Conjugate Gradient Stabilised method (BICGSTAB) [16] using a SIP preconditioner was used for the Poisson pressure correction equation. The solver is computationally efficient, with each of Eqs. (1) and (2) and the Poisson pressure correction equation, being solved only once per time step. Convergence criteria were applied to ensure that the divergence was kept

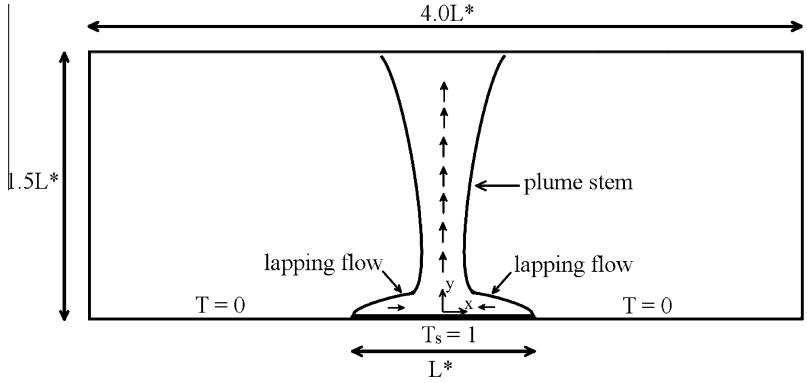

Fig. 1. Computational domain. (The z direction is out of the page. The domain size in the z direction is $0.5L^*$.)